

INTENSITY MEASUREMENTS IN THE
SPECTRUM OF MANGANESE*

BY RAYMOND S. SEWARD

PHYSICAL LABORATORY OF STANFORD UNIVERSITY

ABSTRACT

Relative intensity measurements have been made for the lines of twenty-five multiplets of manganese, containing about one hundred and fifty lines in all. All but three of these were of Mn I. None of the Mn II multiplets measured were found to contain lines of abnormal intensity. On the other hand, at least eight multiplets of Mn I contain lines which are clearly anomalous. These eight multiplets contain a large number of the strongest lines of the spectrum. All involve terms derived from the term a^5D of Mn II and are of the inverted type with wide separations between the subterms. There seems to be regularity in the departure from normal intensities which can best be described by graphs in which the calculated intensities are plotted against the measured intensities on double logarithmic paper. In these plots, the satellites often assume a regular pattern above or below the main diagonal lines.

The total relative intensities of seventeen of these multiplets have also been measured. After reasonable excitation corrections have been applied, the agreement of their intensities with the theoretical values is as close as is to be expected. The measurements on the quartet triad of this group are the most reliable.

INTRODUCTION

THE elements of the iron group present complex spectra which are at present in the process of analysis.¹ A number of intensity studies have been made upon elements of this group, chiefly by Frerichs² at Bonn, by Harrison and co-workers³ at Stanford, and by Ornstein and Bouma⁴ at Utrecht.

The element manganese stands at the center of the iron group. Its maximum multiplicity is eight, which is the largest attained in this group. It is expected that departures from the Russell-Saunders or LS coupling which predominates in elements on the left side of the periodic table will gradually increase as the atomic number of the element in the group becomes greater, and at the same time departures from the normal intensity formulas will increase. Hesthal has found a greater fraction of anomalous lines in the multiplets of chromium ($Z = 24$) than has Harrison in titanium (22), while the work of Ornstein and Bouma indicates still greater departures for cobalt (27) and nickel (28). The element manganese ($Z = 25$) thus takes an interesting intermediate position in this connection.

* This work was done while the author was on leave of absence from the College of Puget Sound.

¹ H. N. Russell, *Astrophys. J.* **66**, 283–328, 347–438 (1927).

² R. Frerichs, *Zeits. f. Physik* **31**, 305 (1925); *Ann. d. Physik* **81**, 807 (1926).

³ G. R. Harrison, *J.O.S.A.* **17**, 389 (1928). G. R. Harrison and H. Engwicht, *J.O.S.A.* **18**, 287 (1929). G. R. Harrison, *J.O.S.A.* **19**, 109 (1929). C. E. Hesthal, Ph.D. Thesis, Stanford University Library. Paper also reported at meeting of Am. Phys. Soc. Chicago, November 29–30, 1929, Paper No. 25. *Abstract Phys. Rev.* **35**, 126 (1930).

⁴ L. S. Ornstein and T. Bouma, *Phys. Rev.* **36**, 679–693 (1930).

Considerable work has been done on the analysis of the spectrum of Mn I and a less amount on that of Mn II. The analysis of Mn I given by McLennan and McLay⁵ and unpublished data furnished by Dunham of Mt. Wilson Observatory have been used in the present study. Material for Mn II has been taken from recent articles by Russell⁶ and by Duffendack and Black.⁷ The assignments of terms to definite electron configurations as given by Russell⁸ and by Hund⁹ is used.

The aim of the present investigation has been to secure accurate intensity determinations of as many lines of the spectrum of manganese as is practicable in order that the information may be available for reference in connection with atomic problems.

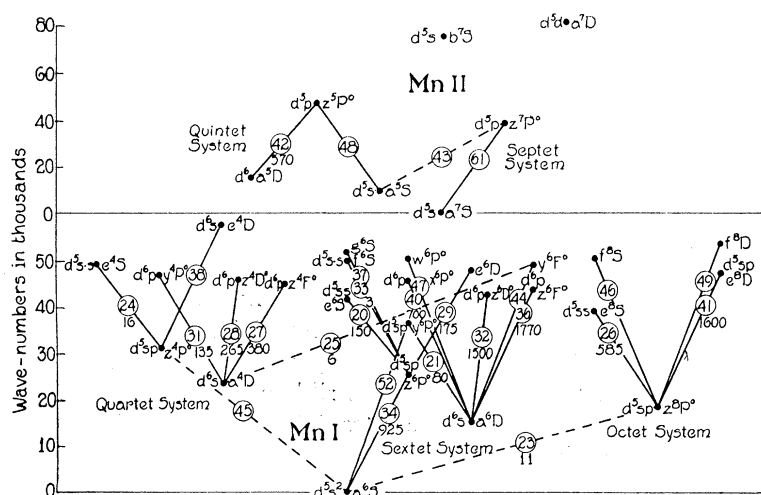


Fig. 1. Energy level diagram of the spectral terms of Mn I and Mn II.

Some features of the manganese spectra are summarized in Fig. 1, which is an energy level diagram of the spectral terms. They are classified according to multiplicity, there being quartet, sextet, and octet terms of Mn I and quintet and septet terms of Mn II. The separations of sub-terms are not shown. Symbols for electron configurations where known are written in front of the term symbols. Lines are drawn between terms to indicate multiplets. These are identified by numbers written in circles drawn on the lines, the larger numbers being assigned to the shorter wave-lengths. Intersystem transitions are represented by dotted lines.

Multiplets 27, 28, and 31 constitute a quartet triad, while multiplets 32, 36, and 40 make up a sextet triad. All six multiplets are due to sp electron

⁵ J. C. McLennan and A. B. McLay, *Trans. Roy. Soc. Canada* **III**, 89 (1926).

⁶ H. N. Russell, *Astrophys. J.* **66**, 233-255 (1927).

⁷ O. S. Duffendack and J. R. Black, *Phys. Rev.* **34**, 35-43 (1929).

⁸ H. N. Russell, *Astrophys. J.* **66**, 283-328, 347-438 (1927).

⁹ F. Hund, *Linienspectren*, Julius Springer, Berlin, 1927, p. 181.

jumps and constitute two related super multiplets. Russell has shown that similar sp jumps are responsible for important triads in other members of the iron group.¹⁰ All of the eight terms involved in these supermultiplets are inverted and will be referred to as the inverted system of terms, while most of the other terms of Mn I are normal. It is in members of this supermultiplet that the most interesting intensity results were found in the present study.

EXPERIMENTAL PROCEDURE

The method of photographic photometry of spectral lines used in the present study has been described thoroughly in an article by G. R. Harrison.¹¹ The general method of procedure will not be given, but only special details noted.

The source used was an arc whose cathode consisted of a purified carbon rod into a cavity of which had been introduced finely pulverized manganese. For the anode a silver rod was used, as this gave a more steady arc than a second carbon rod, there being no serious overlapping of the silver lines with those of manganese.

Some spectrograms on each plate were exposed with an arc run at atmospheric pressure, while for others the pressure was reduced to from 10 to 20 cm of mercury. Currents of from 0.5 to 3.0 amperes were employed in order to give variable conditions of self-reversal and excitation and to bring out the strong and weak lines at the best intensities for measurement.

The source used for calibration in the ultraviolet was a mercury arc in quartz operated by a 110 volt storage battery, while in the visible a gas-filled 6 volt, 20 ampere tungsten lamp with a ribbon filament was used. As a standardizing source for much of the ultraviolet as well as all of the visible, a "black body" electric furnace with quartz window operated at about 2400°C was employed (see page 290 of reference 9), the intensities for various wavelengths being determined by Wien's Law.

For varying the intensity during calibration, neutral wire screens were used whose transmitting power had been previously determined by thermopile readings.

The spectrographic arrangement, as in previous studies, was of a modified Paschen type. The lens for focusing the source on the slit was a quartz fluorite achromat of 2.5 cm aperture and a focal length remarkably constant at about 25 cm for all wave-lengths encountered. The grating was a concave reflector of about 35 feet radius, containing about 85,000 lines, 5900 per cm, the dispersion in the first order being about 1.67 Å. per mm. This grating is remarkably free from ghosts, has intense first and second order spectra, and is in general excellent for intensity work.

The plates used, except for the region $\lambda\lambda$ 5300–6000, were the Eastman 36 brand. To secure measurable spectrograms for the green and yellow regions with the same exposure times as were used for the more actinic regions, panchromatic plates sensitized with ammonia were employed. Such plates, while

¹⁰ See reference 1.

¹¹ G. R. Harrison, J.O.S.A. **19**, 267 (1929).

comparatively sensitive, are apt to become fogged and mottled. Their contrast was found much greater than desired, and the measurements made by their use are not so reliable as the others.

Self-reversal seems to have been reduced to a negligible amount in most cases, as indicated by a 45° slope to the "self-reversal curve" for a multiplet.¹² Exceptions in which self-reversal corrections were added are noted in the discussion of results.

Six sets of plates were secured, two of which covered the entire available spectrum (λ 2500–6000). From 12 to 18 measurable spectra were obtained on

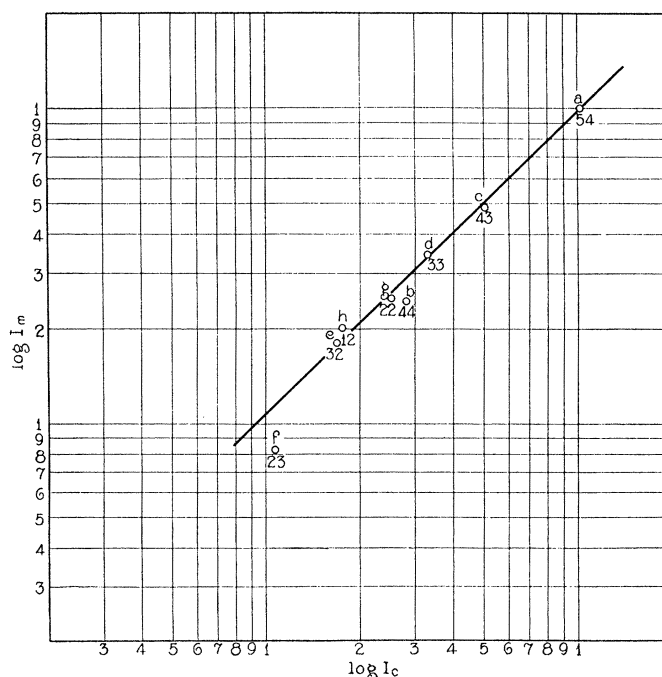


Fig. 2. Calculated and measured intensities for Multiplet 21 ($a^6D - y^6P$).

each plate. The results (recorded in the Table of Results) were obtained by averaging what were considered the most reliable determinations. It was impossible to measure accurately the weaker lines in certain exposures and in others the stronger lines were too black for accurate determination. But from 20 to 60 determinations were made for all but a few inaccessible lines.

RESULTS AND DISCUSSION

Intensities within multiplets. The intensities of the lines making up a given multiplet may be determined with much greater accuracy than is possible when lines of different multiplets are compared, because excitation conditions

¹² In a self-reversal curve, the measured intensities are plotted against the calculated intensities on double logarithmic paper. For an explanation of such curves see p. 401 of the first reference cited in reference 3.

are similar for the various lines, and the plate sensitivity generally does not differ greatly for the lines being compared.

The results of the relative intensity measurements for the individual multiplets are found in column 5 of the Table of Results; the corresponding calculated intensities appear in column 4; while the results obtained by Freirichs for five multiplets which he measured appear in column 6. In all cases the intensity is expressed in percent of the strongest line. For convenience in testing the Sum Rule, the sums of the line intensities from a given upper state and of those having a given lower state have also been determined. These appear in the same column as the line intensities. Column 3 gives the term or transition distinguishing the sum or line.

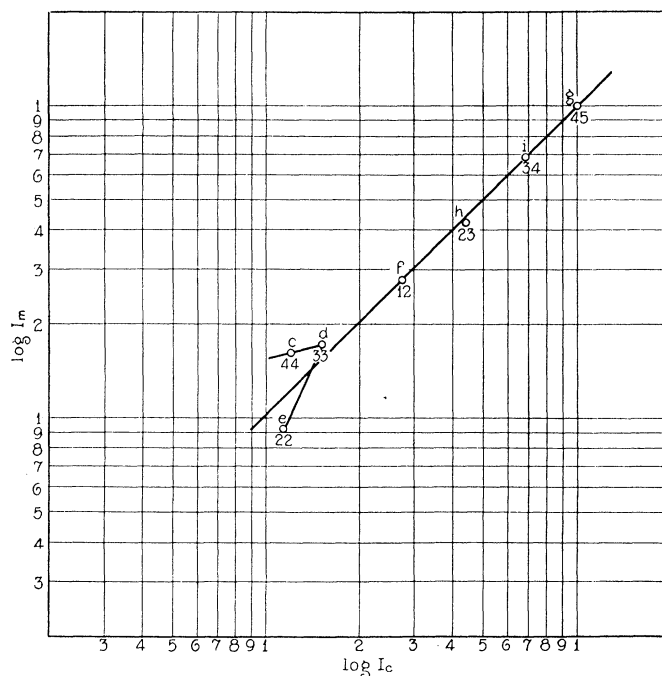


Fig. 3. Calculated and measured intensities for Multiplet 27 ($a^4D - z^4F$).

The measurements for the most interesting individual multiplets will now be discussed, following the order of decreasing wave-length.

Multiplet 21 ($a^6D - y^6P$; $\lambda\lambda$ 5540-5340). Besides lying in a region to which the ordinary photographic emulsion is insensitive, this multiplet covers a wide wave-length range in which the sensitivity of the panchromatic plate has a number of maxima and minima. It was also necessary to use exposures which were not favorable to complete removal of self-reversal. In obtaining the tabular values, self-reversal corrections were applied in some cases. The results indicate that lines b and f are abnormally weak. The multiplet is of interest in that its upper state belongs to the normal system of terms, while its lower state belongs to the inverted system. The calculated and measured intensities are shown graphically in Fig. 2.

Multiplet 23 (a^6S-z^8P ; $\lambda\lambda$ 5432-5395). The two lines in this intersystem multiplet are fairly strong. Although there is no theoretical relation known between the intensities of such lines, the present measurements illustrate that the lines of largest J values are the strongest, and that the intensities follow qualitatively rules similar to those for lines in normal multiplets.

Multiplet 25 ($a^4D_3-z^6F_4, a^4D_4-z^6F_5$; λ 5000) and *Multiplet 45* (a^6S-z^4P ; λ 3220) gave similar results.

Multiplet 27 (a^4D-z^4F ; $\lambda\lambda$ 4766-4671). A large number of very consistent determinations were made on multiplet 27 in which self-reversal graphs showed a uniform slope of 45° , indicating the vanishing of this effect. The averaged values taken from the Table of Results are plotted in Fig. 3. A

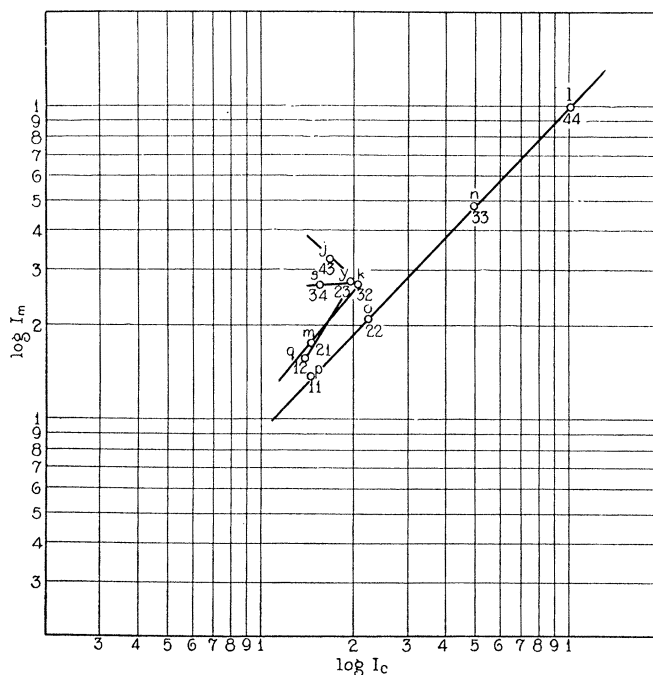


Fig. 4. Calculated and measured intensities for Multiplet 28 (a^4D-z^4D).

large number of similar graphs for the individual exposures showed an almost identical structure. While the four brightest lines are seen to have intensities very close to their calculated values, this is not the case for the first order satellites, line c being much too bright, line d less so, while line e is too weak. The wide divergence of lines c and e which are of nearly equal calculated intensity, is most striking.

Multiplet 28 (a^4D-z^4D ; $\lambda\lambda$ 4502-4415). This multiplet is a second member of the triad to which multiplet 27 belongs. It is also one of the five manganese multiplets measured by Frerichs. As in the previous case, a large number of consistent determinations was made. The plot of the calculated and measured intensities on double logarithmic paper is shown in Fig. 4.

Both groups of satellites show very striking departures from the normal, being too bright by varying amounts. There are eight lines of fairly nearly equal calculated intensity in this multiplet, so that departures from the normal intensity could not very well be explained by self-reversal, even if some were present. An excitation correction would not tend to lessen the departures of the lines, since the lines which are too bright do not have a common upper state.

Multiplet 29 ($z^6P - e^6D$; $\lambda\lambda$ 4462-4455). This is the most satisfactory example of a multiplet belonging to the normal system of Mn I as distinguished from the inverted system. All the lines except *t* and *u* were resolved. The

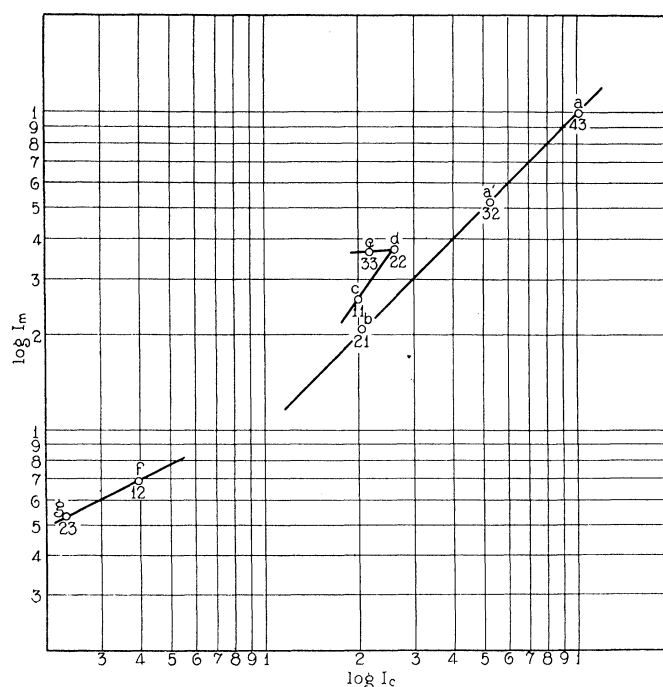


Fig. 5. Calculated and measured intensities for Multiplet 31 ($a^4D - y^4P$).

determinations showed excellent consistency and agreement with the calculated values. Frerichs obtained similar results.

Multiplet 31 ($a^4D - y^4P$; $\lambda\lambda$ 4312-4235). Multiplet 31, plotted in Fig. 5, is the third member of the quartet triad. As in the case of multiplet 28, the first order satellites are too bright; also lines *c* and *e* of nearly equal calculated intensities differ widely in measured intensities. The two second order satellites appear somewhat too bright and of more nearly equal intensities than their calculated values, although these lines were too weak for best determination. Frerichs obtained similar results in this case also.

Multiplet 32 ($a^6D - z^6D^0$; $\lambda\lambda$ 4084-4018). This is the first member of the sextet triad belonging to the sp inverted supermultiplet. Fig. 6 shows some

of the satellites too weak as compared with the main diagonal lines. This is in contrast to the corresponding DD^0 quartet multiplet 28, in which the corresponding lines were too intense. Lines j and k were not resolved completely. Their sum was measured, and then this value was distributed to the two lines in a ratio equal to the apparent intensities given when they were partly resolved. The position of these two individual lines is not known exactly, but their sum is not so great as the calculated value of the sum. This is another case in which departure from calculated values could not be explained by self-reversal, since a number of lines of nearly equal calculated intensities give radically different measured values.

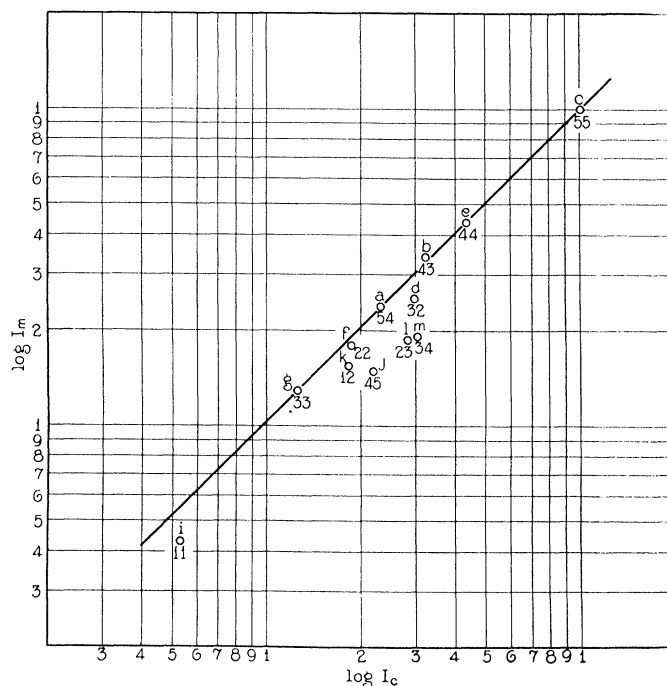


Fig. 6. Calculated and measured intensities for Multiplet 32 ($a^6D - z^6D^0$).

Multiplet 36 ($a^6D - z^6F$; $\lambda\lambda$ 3844–3776). When conditions were best for removal of self-reversal, cyanogen bands were apt to develop in the position occupied by multiplet 36. In order to resolve two pairs of interesting lines, it was also necessary to work in the second order. For these reasons, exposures in which some self-reversal remained were used in calculating the intensities, a small correction being applied to correct for the effect. The plot of the intensities as shown in Fig. 7 would be very similar if this correction had not been applied, except that the slope of the curve would be less. The departures from normal intensities are in this case the clearest and most regular of any so far encountered. The first order satellites are all clearly too weak as compared with the main diagonal lines. Since the lines are too weak, there

is no possibility of explaining their deviations by laps with unidentified lines. The two second order satellites f and i seem to have the order of their intensities inverted, though the data so far as this is concerned are not conclusive.

Multiplet 40 (a^6D-x^6P ; $\lambda\lambda$ 3629-3577). This multiplet completes the sp sextet triad and is the last member of one of the supermultiplets arising from the a^5D term of Mn II. Measurements were possible in which self-reversal was apparently completely eliminated, and a large number of determinations gave nearly identical results. Of the first order satellites, line d is much too intense, line e slightly so, and line f is apparently about normal. The second order satellites g, h, i seem to be abnormally bright; these latter form a line in Fig. 8 which has much less slope than the main diagonal line.

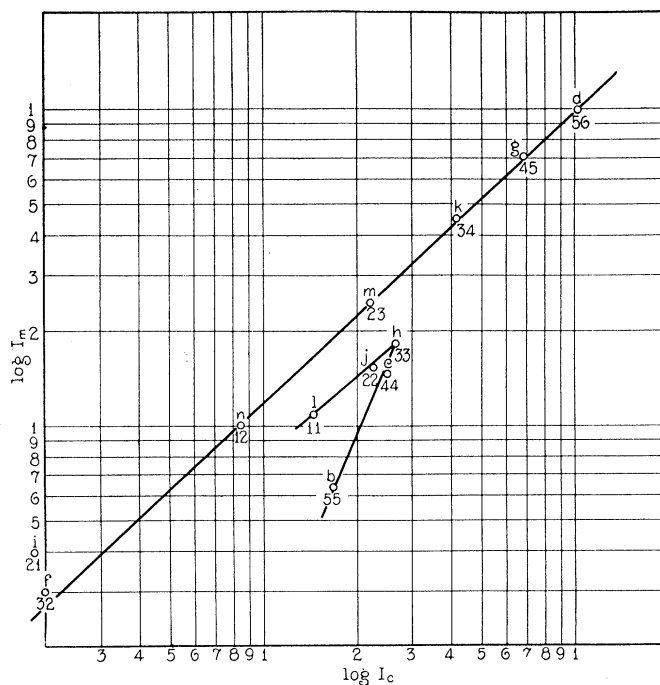


Fig. 7. Calculated and measured intensities for Multiplet 36 (a^6D-z^6F).

Multiplet 42 (a^5D-z^5P ; $\lambda\lambda$ 3497-3442). This was the only complex multiplet of Mn II available for measurement. All measurements gave excellent agreement with the calculated values.

Multiplet 44 ($a^6D-y^6F^0$; $\lambda\lambda$ 3260-3209). Because of its comparative weakness, this multiplet, like its prototype number 36, was measured from exposures which had some self-reversal. The plot of its intensities shown in Fig. 9 is almost a reproduction of that for number 36, except that line f is a little depressed. Although the departure from normal intensities by the first order satellites is of the same type as in number 36 the amount of this departure is somewhat less. The second order satellites seemed to be stronger than their calculated values.

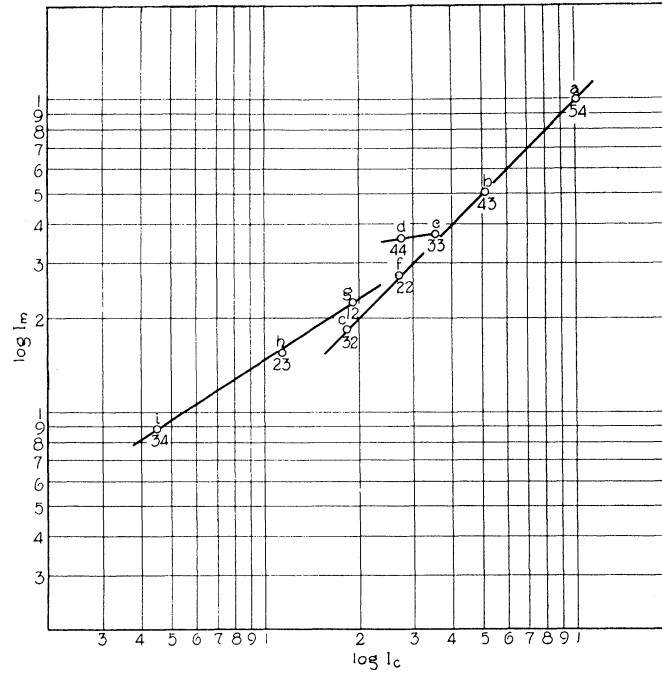


Fig. 8. Calculated and measured intensities for Multiplet 40 ($a^6D - x^6P_4$).

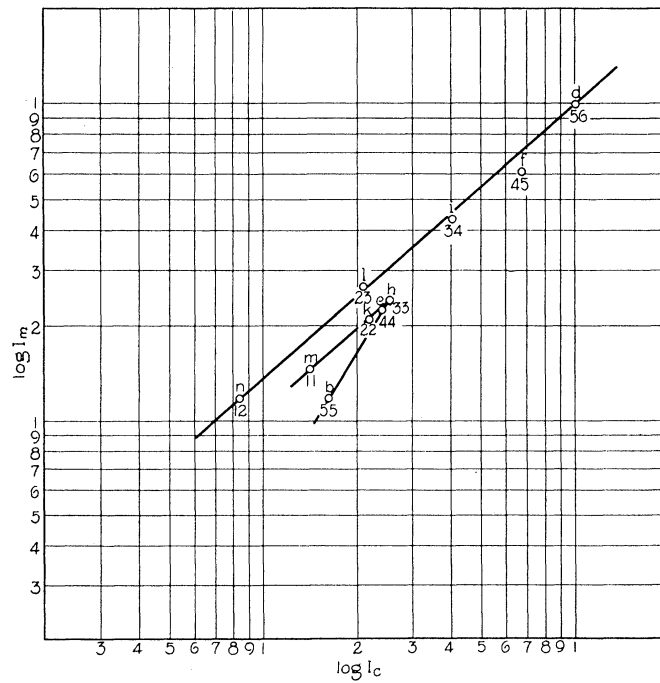


Fig. 9. Calculated and measured intensities for Multiplet 44 ($a^6D - y^6F^0$).

Multiplet 46 (z^3P-f^3S ; $\lambda\lambda$ 3178–3148). Multiplet 46 gave very close agreement with the calculated values. It is the second member of a sharp series following a Rydberg formula, multiplet 26 being the first member.

Multiplet 47 (a^6D-w^6P ; $\lambda\lambda$ 3082–3044). This has the same final state as has number 40. While the upper state has not been assigned to any electron configuration, it has normal intensities or nearly so (Fig. 10), and does not show anomalies analogous to those in number 40.

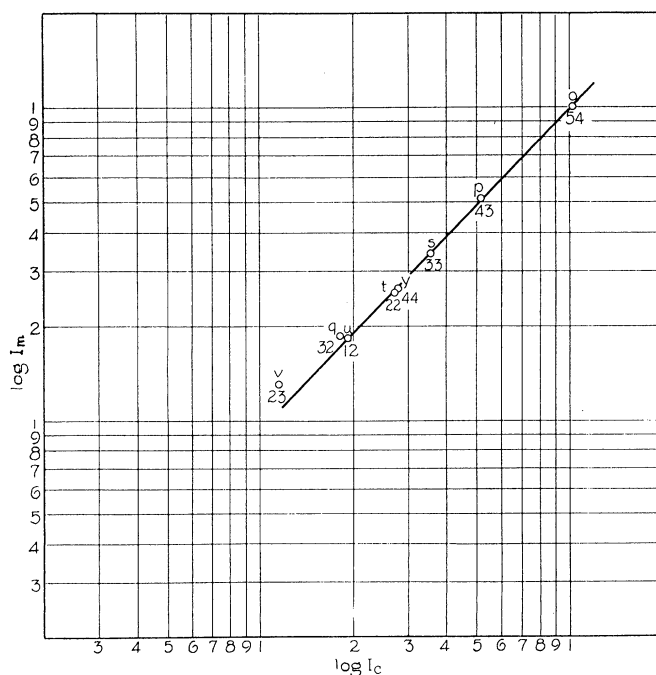


Fig. 10. Calculated and measured intensities for Multiplet 47 (a^6D-w^6P).

Multiplet 49 (z^3P-f^3D ; $\lambda\lambda$ 2940–2914). Measurements indicated the normal intensity ratio between lines *b* and *a*. Line *c* was a little strong, probably due to a lap.

In summarizing the line intensities within multiplets, it may be stated that most of the anomalous lines, if not all of them, were in multiplets whose terms, one or both, were derived from the a^5D term of Mn II. The departure from normal intensities shown in graphs of Figs. 2 to 10 are of a regular nature in some cases at least. It is always possible to draw a straight line which passes through or near each point representing a main diagonal spectral line. Such lines can also be drawn through some of the satellite points, but the latter line is usually broken in the middle. One may proceed along this broken line in the shape of a *V* with the *J* values (subscripts) increasing or decreasing in regular sequence. Lines l_{11} , j_{22} , h_{33} , e_{44} , and b_{55} of multiplet 36 illustrate this regularity. It seems probable that this regular departure is caused by some perturbation factor which is usually negligible but which assumes significant values in the present case.

Relative intensities of the multiplets. Intensities for different multiplets, even when related, depend greatly on excitation conditions; so that measurements obtained under one set of conditions may not be compared directly with those obtained under another set. The figures for relative line and multiplet intensities given in column 7 of the Table of Results are based mainly on measurements made under fairly uniform conditions; namely, a current of 1.0 ampere and a pressure of 18 cm of mercury. Figures for each exposure were worked out separately and reduced to a common standard before finding the average figure which appears in column 7.

To obtain the intensities for infinite excitation as given in column 9, it was necessary to find the equivalent temperature. For this purpose the theoretical intensities of the members of the sp supermultiplet were employed.

The numbers 14, 10, 6, 15, 21, 9 are the intensities of multiplets 27, 28, 31, 32, 36, and 40 respectively as calculated by formula. The calculated intensities for the lines in each multiplet were first adjusted so that their sums were proportional to these numbers. The proper ν^4 correction was applied for each line, and the results placed in column 8 of the Table of Results.

If the multiplets may be brought to their calculated intensities by excitation correction, the equation $\log_{10}R = 0.625\Delta\sigma/T$ must have a common temperature solution. R is the factor required to bring the relative intensity of a line, or group of lines of common upper state, to the value for infinite excitation, and $\Delta\sigma$ is the difference in term values of the upper state in question and that of a line used as a standard.

In seeking the common solution of the above equation, the following procedure may be followed. The ratio I_m/I_c (measured intensity)/(calculated intensity) for each line group of common upper state is determined. The factor R_m by which each of these I_m/I_c values must be multiplied to make it equal to the value for the standard is next found. Finally the logarithms of these R_m values are plotted as ordinates and the corresponding $\Delta\sigma$ values as abscissas. In case these points all lie on a straight line, the intensities are normal, and the equivalent temperature may be found from the slope of this line; i.e., $T = 0.625\Delta\sigma/\log_{10}R$. In practice, a straight line which passes through as many such points as possible is drawn, the equivalent temperature and the corresponding excitation factors for different states being taken as determined by this line, the corrected measured intensities thus coming out greater or less than their calculated values according as their plotted points lie below or above the line.

In the present case, the first four multiplets had intensities which approximated their theoretical values quite closely, the equivalent temperature being between 5000 and 6000A. On the other hand, multiplets 36 and 40 had intensities which were much too small. These multiplets occur at wave-lengths about 3800A and 3600A respectively. It was thought that the apparent anomaly might be due to small J/I standardization values resulting from the action of scattered light. To test this point the values obtained when a filter was used which transmitted only ultraviolet light were tried for the members of the sextet triad, the quartet members being in a region not transmitted by

this filter. In this case the three multiplets showed fair alignment, although the calculated temperature tended to be a little less than in corresponding exposures for the quartet triad.

The measured intensities corrected for infinite excitation as recorded in column 9 of the Table of Results were obtained by first determining the relative intensities of the four multiplets of longest wave-length; then the relative intensities of the three short wave multiplets were determined from two exposures using the filter as just described. The two determinations were then tied together by multiplet 32 common to both sets. The intensities of other short wave multiplets in column 8 were also raised to correspond to these new determinations, the procedure being equivalent to a new standardization. From the preceding statements, it may be inferred that the determinations for the long wave-lengths are most reliable, and that it will be desirable to make further measurements in the ultraviolet in which more reliable standardizations for this region are available. This does not, however, affect the validity of line measurements in multiplets.

No total multiplet intensities for wave-lengths less than 3400A have been given, as intensity values for standardizing are not available at this time.

The approximate multiplet intensities as recorded in column 7 have also been written on Fig. 1, which may be used as a convenient means of studying the multiplet intensities as a whole. The values for the high upper states will be increased, of course, for higher equivalent temperatures or decreased for lower equivalent temperatures than that of the source here employed. It may be noticed that the sextet and quartet triads furnish a large part of the total radiation. Multiplet 41 in the octet system is very intense. Multiplet 34, furnishing the *raies ultimes*, while of very respectable intensity, is nevertheless surpassed by some of the others in total intensity. The comparatively small intensity of multiplet 21 as compared with that of number 40 with the same lower state and higher upper state is of interest. It may be recalled that number 21 has its lower state in the inverted system of terms and upper state in the normal system. Its comparative weakness may be connected with this fact. Multiplet 20, on the other hand, is much more intense than number 33 which has the same lower state. In this case, both the upper states, as well as the lower state, are of the normal type.

The present work has been made possible by the use of the equipment developed by Dr. George R. Harrison in the Stanford Spectroscopy Laboratory. To him and to the other workers in the same laboratory, who have furnished invaluable help and shown a fine spirit of cooperation, the writer wishes to acknowledge his sincere appreciation.

TABLE OF RESULTS. *Summary of intensity measurements.*

Explanation

- Column 1—Number of multiplet; distinguishing letter for each line.
- Column 2—Approximate wave-length of the line.
- Column 3—The transition for the spectral line or the term common to a line sum. Landé quantum numbers are used for the Mn I multiplets or for those of even multiplicity. Sommerfeld quantum numbers are used for Mn II multiplets. The first kind of quantum number is changed into the second by the subtraction of a half unit.

Column 4—Calculated intensity in percent of the strongest line.
 Column 5—Measured intensity in percent of the strongest line.
 Column 6—Intensity in percent of the strongest line as measured by Frerichs.
 Column 7—Measured intensities reduced to a common standard (equivalent temperature about 5500 A, current 1.0 ampere, pressure 18 cm of Hg).
 Column 8—Calculated intensities for six related multiplets reduced to a common standard.
 Column 9—Measured intensities corrected for infinite excitation.

1 No.	2 Mul.	3 Wave-length	4 Trans.	5 I_c in %	6 I_m in %	7 I_f in %	8 I_m St.	9 $I_c \infty$	10 $I_m \infty$
20	c	6021.8	$z^6P_{1/2}e^6S$	100.0	100.0±		65.0		
	b	16.6	$z^6P_{3/2}e^6S$	75.2	75.5±		49.0		
	a	13.5	$z^6P_{5/2}e^6S$	54.3	53.0±		34.4		
20		Total		229.5	228.5		148.4		
21	h	5537.7	$a^4D_{1/2}y^6P_{3/2}$	17.3	20.2		5.7		
	g	16.8	$a^4D_{3/2}y^6P_{3/2}$	25.0	25.0		7.0		
	f	08.9	$a^4D_{5/2}y^6P_{3/2}$	10.6	8.3		2.3		
	e	5481.4	$a^4D_{3/2}y^6P_{5/2}$	16.8	18.3		5.1		
	d	70.6	$a^4D_{5/2}y^6P_{5/2}$	33.0	34.4		9.6		
	c'	57.5	$a^4D_{3/2}y^6P_{7/2}$	4.36	—		—		
	c	20.4	$a^4D_{5/2}y^6P_{7/2}$	49.5	48.3		13.5		
	b	01.4	$a^4D_{3/2}y^6P_{7/2}$	27.2	24.5		6.9		
	a	5341.1	$a^4D_{5/2}y^6P_{7/2}$	100.00	100.0		28.0		
			a^4D_6	100.0	100.0				
			a^4D_4	75.6	72.8				
			a^4D_2	54.1	57.0				
			a^4D_3	35.6	33.3				
			a^4D_1	17.3	20.2				
			$y^6P_{3/2}$	132.0	129.0±				
			$y^6P_{5/2}$	92.0	91.0				
			$y^6P_{7/2}$	58.0	63.5				
21		Total		283.0	283.4		79.0		
23	n	5432.6	$a^4S_{3/2}z^6P_3$		62.7		4.4		
	m	5394.7	$a^4S_{5/2}z^6P_4$		100.0		7.0		
23		Total			162.7		11.4		
24	z	5413.7	$z^4P_{1/2}e^4S$	32.5	34.2		2.7		
	y	5399.5	$z^4P_{3/2}e^4S$	65.8	64.0		5.1		
	x	77.6	$z^4P_{5/2}e^4S$	100.0	100.0		8.0		
24		Total		198.3	198.2		15.8		
25	q	5004.9	$a^4D_{3/2}z^4F_{3/2}$		63.0		2.3		
	p	4965.9	$a^4D_{5/2}z^4F_{3/2}$		100.0		3.7		
25		Total			163.0		6.0		4.5
26	z	4823.5	$z^8P_{1/2}e^8S$	100.0	100.0		240.0		
	y	4783.4	$z^8P_{3/2}e^8S$	82.6	82.5		198.00		
	x	61.5	$z^8P_{5/2}e^8S$	63.2	58.3		140.00		
26		Total		245.8	239.6		578.0		
27	i	4766.4	$a^4D_{3/2}z^4F_{3/2}$	68.0	69.0		92.7	92.6	92.7
	h	4765.9	$a^4D_{5/2}z^4F_{3/2}$	44.5	42.7		57.4	60.7	57.4
	g	62.4	$a^4D_{7/2}z^4F_{3/2}$	100.0	100.0		134.2	136.3	134.2
	f	61.5	$a^4D_{5/2}z^4F_{5/2}$	27.8	27.9		37.5	38.0	37.5
	e	39.1	$a^4D_{7/2}z^4F_{5/2}$	11.4	9.3		12.6	15.6	12.6
	d	27.5	$a^4D_{5/2}z^4F_{7/2}$	15.3	17.3		23.2	20.8	23.2
	c	09.7	$a^4D_{7/2}z^4F_{7/2}$	12.1	16.3		21.9	16.5	21.9
	b	01.2	$a^4D_{5/2}z^4F_{9/2}$.85	.7±		.94	1.15	.94
	a	4671.7	$a^4D_{7/2}z^4F_{9/2}$.6	.6±		.81	.82	.81
			a^4D_4	113.	116.9			153.6	
			a^4D_3	84.	87.0			114.6	
			a^4D_2	56.	52.0			76.1	
			a^4D_1	27.8	27.9			38.	
			$z^4F_{3/2}$	100.0	100.0		134.2	136.3	134.2
			$z^4F_{5/2}$	80.0	85.3		114.6	109.1	114.6
			$z^4F_{7/2}$	60.3	60.6		81.4	82.3	81.4
			$z^4F_{9/2}$	39.7	40.05		51.0	54.7	51.0
27		Total		280.0	286.0		381.25	382.0	381.25

1 No.	2 Mul.	3 Wave-length	4 Trans.	5 I_c in %	6 I_m in %	7 I_f in %	8 I_m St.	9 $I_c \infty$	10 $I_m \infty$	
28	s r q p o n m l k j	4502.2	$a^4D_{32}z^4D^0_4$	15.6	27.0	24.5	21.6	19.2	32.4	
		4498.9	$a^4D_{22}z^4D^0_3$	19.7	27.6	23.6	22.1	24.2	36.1	
		90.1	$a^4D_{12}z^4D^0_2$	14.0	15.7	14.5	12.6	17.2	18.8	
		72.8	$a^4D_{12}z^4D^0_1$	14.4	13.9	12.4	11.1	17.5	16.7	
		70.1	$a^4D_{22}z^4D^0_2$	22.6	21.0	17.6	16.8	27.8	25.2	
		64.7	$a^4D_{22}z^4D^0_1$	49.5	48.0	40.5	38.4	61.0	57.6	
		53.0	$a^4D_{32}z^4D^0_1$	14.5	17.3	15.7	13.8	17.8	20.7	
		51.6	$a^4D_{42}z^4D^0_1$	100.	100.0	100.	80.0	123.	120.0	
		36.4	$a^4D_{32}z^4D^0_2$	20.8	27.2	25.4	21.8	25.6	32.6	
		14.9	$a^4D_{42}z^4D^0_1$	16.9	32.4	26.6	25.9	20.8	39.8	
				a^4D_4	116.9	132.4	126.6		143.8	
				a^4D_3	85.9	102.0	90.4		105.8	
				a^4D_2	56.8	65.9	56.9		69.8	
				a^4D_1	28.4	29.6	26.9		34.7	
		$z^4D^0_4$	115.6	127.0	124.5	101.6	142.2	152.4		
		$z^4D^0_3$	86.1	108.0	90.7	86.4	106.	133.5		
		$z^4D^0_2$	57.4	63.9	57.5	51.2	70.6	76.6		
		$z^4D^0_1$	28.9	31.1	28.1	24.9	35.3	37.4		
28		Total	288.0	330.0	300.8	264.1	354.1	400.0		
29	B ∞ z y x w v u t	4462.0	$z^6P_{46}e^6D_6$	100.0	100.0	100.0	57.0			
		61.1	$z^6P_{46}e^6D_4$	28.6	29.1	26.9	16.6			
		60.4	$z^6P_{46}e^6D_3$	4.76	6.8±	4.64	3.9			
		58.3	$z^6P_{36}e^6D_4$	51.6	51.8	51.8	29.6			
		57.6	$z^6P_{36}e^6D_3$	36.6	37.9	37.2	21.1			
		57.0	$z^6P_{36}e^6D_2$	12.0	11.6	11.4	6.6			
		55.8	$z^6P_{36}e^6D_1$	18.6	18.4	17.3	10.5			
		58.3	$z^6P_{26}e^6D_3$	28.5	27.8	26.9	15.8			
		55.0	$z^6P_{26}e^6D_1$	20.1	22.7	18.9	12.9			
				$z^6P^0_4$	133.4	135.9	131.5			
				$z^6P^0_3$	100.2	100.4	100.4			
				$z^6P^0_2$	67.22	68.9	63.1			
				e^6D_6	100.0	100.0	100.0			
				e^6D_4	80.2	80.9	78.7			
		e^6D_3	60.0	62.4	59.1					
		e^6D_2	40.5	39.4	38.3					
		e^6D_1	20.1	22.7	18.9					
29		Total	300.8	305.2	295.0	174.0		400.0		
31	g f e d c b a a	4312.6	$a^4D_{34}V^4P^0_3$	2.32	5.4±	6.7	2.5	2.44	5.2	
		4284.1	$a^4D_{34}V^4P^0_2$	3.94	6.9±	7.1	3.3	4.14	6.7	
		81.1	$a^4D_{34}V^4P^0_1$	21.4	36.4	34.6	17.2	22.5	35.4	
		65.9	$a^4D_{24}V^4P^0_3$	25.8	37.3	32.5	17.6	27.1	36.3	
		57.7	$a^4D_{24}V^4P^0_2$	20.0	26.2	23.4	12.8	21.05	25.5	
		39.7	$a^4D_{24}V^4P^0_1$	20.6	21.0	20.8	9.8	21.7	20.4	
		35.3	$a^4D_{14}V^4P^0_3$	100.0	100.0	100.0	47.1	105.0	97.2	
		35.1	$a^4D_{14}V^4P^0_2$	62.3	52.3	52.3	24.7	54.9	51.0	
				a^4D_4	100.0	100.0	100.0		105.0	
				a^4D_3	73.7	88.7	87.1		77.4	
				a^4D_2	48.7	63.7	60.0		51.2	
				a^4D_1	23.9	33.1	30.5		25.2	
				$\gamma^4P^0_4$	123.7	141.8	141.3	66.8	129.9	137.8
				$\gamma^4P^0_3$	82.0	96.5	92.1	45.6	86.1	94.0
		$\gamma^4P^0_1$	40.6	47.2	44.2	22.6	42.7	45.9		
31		Total	246.3	285.5	277.6	139.8	258.8	277.7		
32	m l k j i h g f e d c b a	4083.6	$a^8D_{38}z^8D^0_4$	30.2	19.2	23.0	87.0	65.1	42.8	
		82.9	$a^8D_{28}z^8D^0_4$	28.5	19.0	21.7	86.0	61.0	42.3	
		79.4	$a^8D_{18}z^8D^0_4$	18.2	15.5	15.0	70.0	39.0	34.5	
		79.2	$a^8D_{18}z^8D^0_3$	21.6	15.0	15.0	68.0	46.1	33.4	
		70.3	$a^8D_{18}z^8D^0_2$	5.3	4.3	4.3	19.5	11.4	9.6	
		68.0	$a^8D_{18}z^8D^0_1$.53	1.1±	.5	5.0	1.14	2.4	
		63.5	$a^8D_{28}z^8D^0_3$	12.3	13.1	13.5	59.4	26.4	29.2	
		58.9	$a^8D_{28}z^8D^0_2$	18.6	18.1	16.8	82.0	39.8	40.3	
		55.6	$a^8D_{28}z^8D^0_1$	43.5	43.9	45.0	198.5	93.0	97.5	
		48.8	$a^8D_{38}z^8D^0_3$	29.4	25.1	29.4	113.8	63.0	55.9	
		41.4	$a^8D_{38}z^8D^0_2$	100.0	100.0	100.0	454.0	214.0	222.0	
		35.7	$a^8D_{38}z^8D^0_1$	32.0	34.3	30.9	155.0	68.4	76.1	
		18.1	$a^8D_{48}z^8D^0_1$	22.9	24.0	23.5	109.0	49.0	53.5	
				a^8D_8	122.9	124.0	123.5		263.0	
		a^8D_4	97.1	93.2	90.9		207.5			
		a^8D_3	71.9	57.4	65.9		154.5			
		a^8D_2	47.6	38.2	39.		101.9			
		a^8D_1	23.5	19.8	19.3		50.4			
		$z^8D^0_4$	121.6	115.0	115.0	522.0	260.1	255.4		

1 No.	2 Mul.	3 Wave-length	4 Trans.	5 I_c in %	6 I_m in %	7 I_f in %	8 I_m St.	9 $I_c \infty$	10 $I_m \infty$
			$z^6D^0_4$	96.6	87.1	91.5	394.5	207.1	193.8
			$z^6D^0_3$	72.8	66.4	66.1	300.4	155.8	147.6
			$z^6D^0_2$	48.1	41.7	44.9	188.8	103.1	92.8
			$z^6D^0_1$	23.9	22.4	21.1	101.5	51.2	49.9
32			Total	363.0	332.6	338.5	1507.0	777.3	739.5
33	<i>r</i>	4061.7	$z^6P^0_4/f^6S$	100.0	100.0±		1.2		
	<i>q</i>	4059.4	$z^6P^0_3/f^6S$	75.0	74.2±		.9		
	<i>p</i>	4057.96	$z^6P^0_2/f^6S$	50.0	50.6±		.6		
33			Total	225.0	224.8		2.7		
34	<i>z</i>	4034.5	$a^6S^0_2P^0_2$	50.0	60.0		206.0		
	<i>y</i>	33.1	$a^6S^0_2P^0_3$	75.0	87.5		309.0		
	<i>x</i>	30.8	$a^6S^0_2P^0_4$	100.0	100.0		412.0		
34			Total	225.	247.5		927.0		
36	<i>n</i>	3844.0	$a^6D_1z^6F^0_2$	8.27	10.1		55.0	33.1	41.0
	<i>m</i>	41.1	$a^6D_2z^6F^0_3$	21.2	24.1		131.0	85.0	98.0
	<i>l</i>	39.8	$a^6D_3z^6F^0_1$	14.2	10.9		59.2	57.0	44.4
	<i>k</i>	34.4	$a^6D_3z^6F^0_4$	40.2	45.2		245.0	161.0	184.0
	<i>j</i>	33.9	$a^6D_2z^6F^0_2$	22.1	15.4		83.6	88.6	62.7
	<i>i</i>	29.7	$a^6D_2z^6F^0_1$	1.81	4. ±		21.7	7.2	16.3
	<i>h</i>	23.9	$a^6D_3z^6F^0_3$	26.0	18.3		99.0	104.0	74.5
	<i>g</i>	23.5	$a^6D_3z^6F^0_6$	66.0	71.1		386.0	264.0	289.0
	<i>f</i>	16.7	$a^6D_3z^6F^0_2$	1.97	3. ±		16.0	7.91	12.2
	<i>e</i>	09.6	$a^6D_4z^6F^0_4$	24.6	14.8		80.5	98.5	60.7
	<i>d</i>	06.9	$a^6D_6z^6F^0_6$	100.0	100.0		543.0	400.0	407.0
	<i>c</i>	3799.3	$a^6D_6z^6F^0_3$	1.36	(2)		11.0	5.45	8.1
	<i>b</i>	90.2	$a^6D_6z^6F^0_6$	16.4	6.5		35.2	65.5	26.4
	<i>a</i>	76.5	$a^6D_6z^6F^0_4$.6	(1)		5.4	2.4	4.1
			a^6D_6	117.0	107.5			417.0	
			a^6D_4	92.0	87.9			368.0	
			a^6D_3	68.2	66.5			272.9	
			a^6D_2	45.1	45.1			180.8	
			a^6D_1	22.5	21.0			90.1	
			$z^6F^0_6$	100.0	100.0		543.0	400.0	407.0
			$z^6F^0_6$	82.4	77.6		421.2	329.5	315.4
			$z^6F^0_4$	65.4	61.0		330.9	261.9	248.3
			$z^6F^0_3$	48.6	44.4		241.0	194.5	180.6
			$z^6F^0_2$	32.4	28.5		154.6	129.6	115.9
			$z^6F^0_1$	16.0	14.9		80.9	64.2	60.7
36			Total	344.8	326.4		1770.0	1379.7	1328.0
38		3800.6	$z^6P^0_2e^6D_4$	100.0	100.0				
		3787.5	$z^6P^0_2e^6D_3$	53.6	40.0±				
		74.7	$z^6P^0_2e^6D_3$	23.2	15.0±				
38			Total	176.8	155.0				
40	<i>i</i>	3629.1	$a^6D_3xz^6P^0_4$	4.5	8.9	13.3	19.7	11.5	23.8
	<i>h</i>	23.8	$a^6D_3xz^6P^0_3$	11.4	15.5	23.6	34.4	29.1	41.4
	<i>g</i>	19.4	$a^6D_3xz^6P^0_2$	19.2	22.3	32.8	49.5	49.0	58.5
	<i>f</i>	10.3	$a^6D_3xz^6P^0_2$	27.4	27.3	40.0	60.5	70.0	72.8
	<i>e</i>	08.5	$a^6D_3xz^6P^0_3$	35.3	37.0	50.3	82.0	90.3	98.8
	<i>d</i>	07.5	$a^6D_3xz^6P^0_4$	27.6	35.9	48.7	79.7	70.7	95.8
	<i>c</i>	3595.1	$a^6D_3xz^6P^0_2$	18.4	18.5	22.5	41.0	46.6	49.4
	<i>b</i>	86.5	$a^6D_3xz^6P^0_3$	51.1	50.4	58.4	112.0	131.0	134.5
	<i>a</i>	77.9	$a^6D_3xz^6P^0_4$	100.0	100.0	100.0	222.0	256.0	267.0
			a^6D_5	100.0	100.0	100.0		256.0	
			a^6D_4	78.7	86.3	107.1		201.7	
			a^6D_3	58.2	64.4	86.1		148.4	
			a^6D_2	38.8	42.8	63.6		99.1	
			a^6D_1	19.2	22.3	32.8		49.0	
			$z^6P^0_4$	132.1	144.8	162.0	321.4	338.2	385.6
			$z^6P^0_3$	97.8	102.9	132.3	228.4	250.4	274.7
			$z^6P^0_2$	65.0	68.1	95.3	151.0	165.6	181.7
40			Total	294.9	315.8	389.6	700.0	754.2	819.2

* Self-reversal not completely eliminated.

1 No.	2 Mul.	3 Wave-length	4 Trans.	5 I_c in %	6 I_m in %	7 I_f in %	8 I_m St.	9 $I_c \infty$	10 $m I \infty$
41		3570.1	$2^8P_{14}e^3D_4$	6.5					
		69.8	$2^8P_{14}e^3D_4$	32.5					
		69.5	$2^8P_{14}e^3D_4$	100.					
		48.2	$2^8P_{14}e^3D_3$	18.5					
		48.0	$2^8P_{14}e^3D_4$	43.2					
		47.8	$2^8P_{14}e^3D_3$	52.2					
		32.1	$2^8P_{14}e^3D_2$	34.8					
		32.0	$2^8P_{14}e^3D_3$	33.4					
		31.8	$2^8P_{14}e^3D_4$	19.0					
			<i>w</i>		2^8P_{14}	139.0			
	<i>v</i>		2^8P_{14}	113.0					
	<i>u</i>		2^8P_{14}	86.5			430.		
41		Total		338.5			1680.		
42	<i>h</i> <i>g</i> <i>f</i> <i>e</i> <i>d</i> <i>c</i> <i>c</i> <i>b</i> <i>a</i>	3497.5	$a^5D_{12}e^2P_{12}$	7.8	7.7		16.2		
		96.8	$a^5D_{12}e^2P_{12}$	3.5	3.9		8.2		
		95.8	$a^5D_{12}e^2P_{11}$	10.4	10.3		22.0		
		86.6	$a^5D_{12}e^2P_{11}$	23.6	23.6		49.5		
		82.9	$a^5D_{12}e^2P_{12}$	31.0	30.5		64.0		
		74.1	$a^5D_{12}e^2P_{11}$	18.7	19.0		40.0		
		74.0	$a^5D_{12}e^2P_{11}$	25.0	25.4		53.4		
		60.3	$a^5D_{12}e^2P_{12}$	50.0	50.1		105.2		
		42.0	$a^5D_{12}e^2P_{12}$	100.0	100.0		210.0		
			a^5D_4	100.0	100.0				
			a^5D_3	75.0	75.4				
			a^5D_2	53.2	53.4				
			a^5D_1	31.4	31.3				
			a^5D_0	10.4	10.4				
	2^8P_{12}	128.5	129.3						
	2^8P_{12}	88.8	88.3						
	2^8P_{11}	52.7	53.0						
42		Total		270.0	270.6		568.5		
44	<i>n</i> <i>m</i> <i>l</i> <i>k</i> <i>j</i> <i>i</i> <i>h</i> <i>g</i> <i>f</i> <i>d</i> <i>c</i> <i>c</i> <i>b</i> <i>a</i>	3260.2	$a^6D_{13}e^2F_{12}$	8.3	11.8				
		58.4	$a^6D_{13}e^2F_{11}$	14.2	14.7				
		56.1	$a^6D_{13}e^2F_{12}$	21.1	26.6				
		52.9	$a^6D_{13}e^2F_{12}$	22.0	21.0				
		51.1	$a^6D_{13}e^2F_{11}$.18	4.5 ±				
		48.5	$a^6D_{13}e^2F_{14}$	40.3	43.8				
		43.8	$a^6D_{13}e^2F_{12}$	25.8	24.1				
		40.6	$a^6D_{13}e^2F_{12}$.2	7. ±				
		36.8	$a^6D_{13}e^2F_{12}$	66.5	61.7				
		30.7	$a^6D_{13}e^2F_{14}$	24.1	22.6				
		28.1	$a^6D_{13}e^2F_{12}$	100.0	100.0				
		26.0	$a^6D_{13}e^2F_{12}$.14	3. ±				
		12.9	$a^6D_{13}e^2F_{12}$	16.4	11.9				
		06.9	$a^6D_{13}e^2F_{14}$.06	—				
			a^6D_5	117.0	112.0				
			a^6D_4	90.7	87.3				
			a^6D_3	66.9	74.9				
			a^6D_2	43.3	52.1				
	a^6D_1	22.5	26.5						
	3^6F_{12}	100.0	100.0						
	3^6F_{12}	82.9	73.6						
	3^6F_{11}	64.5	66.4						
	3^6F_{11}	47.0	53.7						
	3^6F_{12}	30.5	39.8						
	3^6F_{11}	14.4	19.2						
44		Total		339.3	352.7				
45	<i>g'</i> <i>x</i>	3224.8	$a^6S_{24}P_{12}$		100.0				
		17.0	$a^6S_{24}P_{12}$		45.0				
45		Total			145.0				
46	<i>m'</i> <i>m'</i> <i>l'</i>	3178.5	$2^8P_{14}f^3S$	100.0	100.0				
		61.1	$2^8P_{14}f^3S$	82.0	82.1				
		48.2	$2^8P_{14}f^3S$	62.2	62.6				
46		Total		244.2	244.7				

1 No. Mul.	2 Wave-length	3 Trans.	4 I_c in %	5 I_m in %	6 I_f in %	7 I_m St.	8 $I_c \infty$	9 $I_m \infty$	
47	w	3082.1	$a^4D_1w^6P^0_4$	4.55	lapped				
	v	81.3	$a^4D_2w^6P^0_4$	11.4					
	u	79.6	$a^4D_1w^6P^0_3$	19.2					
	t	73.1	$a^4D_2w^6P^0_3$	27.2					
	s	70.3	$a^4D_3w^6P^0_3$	35.2					
	r	66.0	$a^4D_4w^6P^0_3$	27.8					
	q	62.1	$a^4D_3w^6P^0_2$	18.2					
	p	54.4	$a^4D_4w^6P^0_2$	51.0					
	o	44.6	$a^4D_5w^6P^0_2$	100.0					
			a^4D_5	100.0					
			a^4D_4	78.8					
			a^4D_3	58.0					
			a^4D_2	38.6					
			a^4D_1	19.2					
		$w^6P^0_4$	132.4						
		$w^6P^0_3$	97.6						
		$w^6P^0_2$	64.6						
		Total	294.6	292.2					
47		Total	294.6	292.2					
	48	z	2949.2	$a^8S_{22}^8P^0_4$	100.0	100.0			
		y	39.3	$a^8S_{22}^8P^0_3$	73.0	72.2			
x		33.1	$a^8S_{22}^8P^0_1$	44.0	43.0				
		Total	217.0	215.2					
49	G	2940.5	$z^8P^0_3f^8D$	100.0	100.0 ± (lap)				
	B	25.6	$z^8P^0_4f^8D$	81.3	81.3				
	A	14.6	$z^8P^0_3f^8D$	62.0	63.8				
		Total	243.3	245.1					
52	c	2801.1	$a^8S_{22}^8P^0_2$	50.0	*100. ±				
	b	2798.3	$a^8S_{22}^8P^0_3$	75.0	90. ±				
	a	94.8	$a^8S_{22}^8P^0_4$	100.0	80. ±				
		Total	225.0						
61		2605.7	$a^7S_{22}^7P^0_3$	47.5	*100. ±				
		2593.7	$a^7S_{22}^7P^0_2$	68.5	100. ±				
		76.1	$a^7S_{22}^7P^0_4$	100.0	100. ±				
		Total	216.0						

* Self-reversal; J/I uncertain.